Published online 13 May 2020

Nucleic Acids Research, 2020, Vol. 48, No. 11 ***5799–5813***
doi: 10.1093/nar/gkaa311

NAR Breakthrough Article

Prp5—Spt8/Spt3 interaction mediates a reciprocal coupling between splicing and transcription

Wei Shao[1,2], Zhan Ding[2,3], Zeng-Zhang Zheng[3], Ji-Jia Shen[1], Yu-Xian Shen[1], Jia Pu[3], Yu-Jie Fan[2], Charles C. Query[4,*] and Yong-Zhen Xu[2,*]

[1]School of Basic Medical Sciences, Anhui Medical University, Hefei, Anhui 230032, China, [2]State Key Laboratory of Virology, Hubei Key Laboratory of Cell Homeostasis, College of Life Science, Wuhan University, Wuhan, Hubei 430072, China, [3]Key Laboratory of Insect Developmental and Evolutionary Biology, Institute of Plant Physiology and Ecology, Chinese Academy of Sciences, Shanghai 200032, China and [4]Department of Cell Biology, Albert Einstein College of Medicine, NY 10461, USA

Received July 30, 2019; Revised April 08, 2020; Editorial Decision April 16, 2020; Accepted May 03, 2020

ABSTRACT

Transcription and pre-mRNA splicing are coupled to promote gene expression and regulation. However, mechanisms by which transcription and splicing influence each other are still under investigation. The ATPase Prp5p is required for pre-spliceosome assembly and splicing proofreading at the branch-point region. From an open UV mutagenesis screen for genetic suppressors of *prp5* defects and subsequent targeted testing, we identify components of the TBP-binding module of the Spt–Ada–Gcn5 Acetyltransferase (SAGA) complex, Spt8p and Spt3p. *Spt8Δ* and *spt3Δ* rescue the cold-sensitivity of *prp5-GAR* allele, and *prp5* mutants restore growth of *spt8Δ* and *spt3Δ* strains on 6-azauracil. By chromatin immunoprecipitation (ChIP), we find that *prp5* alleles decrease recruitment of RNA polymerase II (Pol II) to an intron-containing gene, which is rescued by *spt8Δ*. Further ChIP-seq reveals that global effects on Pol II-binding are mutually rescued by *prp5-GAR* and *spt8Δ*. Inhibited splicing caused by *prp5-GAR* is also restored by *spt8Δ*. *In vitro* assays indicate that Prp5p directly interacts with Spt8p, but not Spt3p. We demonstrate that Prp5p's splicing proofreading is modulated by Spt8p and Spt3p. Therefore, this study reveals that interactions between the TBP-binding module of SAGA and the spliceosomal ATPase Prp5p mediate a balance between transcription initiation/elongation and pre-spliceosome assembly.

INTRODUCTION

Eukaryotic mRNA processing consists of multiple steps that occur in the nucleus after transcription, including 5′-capping, pre-mRNA splicing, 3′-polyadenylation, and RNA modifications, which occur mostly co-transcriptionally, and subsequent post-transcriptional steps of mRNA export and RNA surveillance (1,2). Although each of these steps can be investigated independently in vitro, much evidence in the past two decades demonstrated that these processes affect each other extensively and that such 'coupling' contributes to gene expression and regulation (reviewed in 3,4–6).

Transcription is central to the coupling of RNA processing events, primarily through the catalytic component, RNA polymerase II (Pol II) (6,reviewed in 7). Removal of introns from nascent transcripts by pre-mRNA splicing is essential in all eukaryotes. Coupling between transcription and splicing has been extensively studied. In one direction, components of the transcription machinery associate with splicing factors and regulate pre-mRNA splicing. For example, RNA Pol II has extensive association with SR proteins and other factors that promote efficient spliceosome assembly (8). The C-terminal domain (CTD) of RNA Pol II recruits SRp20, promotes exon skipping, and regulates alternative splicing (9). RNA Pol II and emergent splice sites in the nascent pre-mRNA are tethered together (10), with spliceosomal components being recruited in part by the Ser5-phosphorylated CTD of Pol II during transcription elongation (11). In the other direction, splicing factors also promote transcription elongation. Depletion of splicing factor SC35 induces RNA Pol II accumulation within the body of specific genes and attenuates transcription elon-

*To whom correspondence should be addressed. Tel: +86 27 68789348; Email: Yongzhen.Xu@whu.edu.cn
Correspondence may also be addressed to Charles C. Query. Tel: +1 718 4304174; Email: charles.query@einsteinmed.org

gation, correlating with defective recruitment of transcription factor P-TEFb and a dramatic reduction of Ser2 phosphorylation of the CTD (12). Recruitment of SR proteins to nascent *FOS* transcript is RNase sensitive and transcription dependent, indicating that SR proteins are not preassembled with Pol II (13). A dual-function factor, Tat-SF1, identified as a transcription elongation factor in humans, interacts with snRNPs and strongly stimulates both polymerase elongation *in vivo* and splicing *in vitro* (14,15).

Two models have been proposed to explain the cotranscriptionality of splicing. The first is 'recruitment coupling', in which splicing factors are recruited by the transcription machinery. For example, the CTD of RNA Pol II directly interacts with a human spliceosomal U2AF65–Prp19 complex (16), and the yeast SR-like protein Npl3p facilitates co-transcriptional recruitment of splicing factors and thereby promotes splicing (17). The second model is 'kinetic coupling', which is achieved by coordinating the rates of transcription and splicing—i.e. the relative rates of sequential events are coordinated to optimize their function. In general, the transcription rate is hindered by chromatin structure, and the splicing rate is dependent on the strength of splice sites and binding of splicing regulators (18). However, transcription rates influence the outcome of splicing (19–21) and splice events also could be transcription checkpoints. Factors such as SC35, SAM68, and the DBC1–ZIRD (DBIRD) complex, which can modulate transcription and splicing rates, are important in the kinetic co-transcriptional model (12,22–25).

Evidence has pointed to U2 snRNP components and its related event, pre-spliceosome assembly, as critical in the process of co-transcriptional splicing. First, two core components of U2 snRNP, Lea1p/U2A′ and Msl1p/U2B″ (yeast/mammalian names), exhibit genetic interactions with *GCN5*; deletion of *GCN5* rescues yeast lethality caused by double deletion of *LEA1* and *MSL1* (26). Gcn5p is a catalytic component of the Spt–Ada–Gcn5 Acetyltransferase (SAGA) complex, an evolutionary conserved, multifunctional transcription co-activator comprising two distinct enzymatic activities, acetylation and deubiquitination of histone residues (27,28). The histone acetyltransferase (HAT) activity of Gcn5p is required for co-transcriptional recruitment of the U2 snRNP (26). Second, Cus2p, a yeast U2 snRNP component and putative orthologue of human Tat-SF1 (29), has been proposed as a potential checkpoint factor in transcription elongation (30). Cus2p has been investigated as a functional target of Prp5p (31,32). Prp5p is a spliceosomal RNA-dependent ATPase required for stable binding of U2 snRNP to the branch site region (BS) and consequent pre-spliceosome assembly (33–36). *PRP5* mutant allele *prp5–1* causes transcriptional defects of intron-containing genes, in which accumulation of RNA Pol II across introns was observed, but this accumulation was relieved in the absence of Cus2p (30). This led to a model wherein Cus2p is a potential transcription elongation checkpoint factor during cotranscriptional spliceosome assembly.

Physical interactions have been reported between components of the SAGA complex and U2 snRNP, each complex containing around 20 subunits, conserved from yeast to mammals. The SAGA complex is important in transcription initiation and elongation, and in mRNA export (37,38). It is organized into four functional modules, including a HAT (histone acetyltransferase) module, a DUB (deubiquitinase) module, a Core structure module, and a TBP-binding module. 17S U2 snRNP is composed of U2A′, U2B″, Sm proteins, SF3a, and the SF3b complex (39). Human SAGA component SPT3 was found to interact with SF3B3/SAP130 (40,41), a subunit in the SF3b complex that is critical for pre-spliceosome assembly (42,43). In *Drosophila*, two SF3b subunits, SF3B3 and SF3B5, are proposed as components of the SAGA complex and interact with multiple SAGA subunits, including Sgf29 and Spt7, in a yeast two-hybrid assay (44).

Multiple genetic and physical interactions between the SAGA complex and U2 snRNP strongly suggest that these two complexes are important for regulation of co-transcriptional splicing. However, the details and mechanisms for how coupling between transcription and splicing is mediated remain unclear. In this study, we performed a genetic screen in yeast and found that a component of transcriptional complex SAGA, *SPT8*, genetically interacts with *PRP5*. Further genetic studies revealed that such interactions are limited to the TBP-binding module of the SAGA complex. We propose that the TBP-binding module (Spt8p/Spt3p) of SAGA, together with the spliceosomal RNA helicase Prp5p, mediate a balance between transcription initiation/elongation and pre-spliceosome assembly/proofreading.

MATERIALS AND METHODS

Yeast strains and plasmids

Saccharomyces cerevisiae strains used in this study are listed in Supplementary Table S1. They were derived from strain *46ΔCUP* (45), yYZX02 (*MATa, ade2 cup1Δ::ura3 his3 leu2 lys2 prp5Δ::loxP trp1,* pRS316-PRP5 [*PRP5 URA3* CEN ARS]), or yYZX06 (*MATa, ade2 cup1Δ::ura3 his3 leu2 lys2 prp5Δ::loxP trp1, cus2Δ::loxP* pRS316-PRP5 [*PRP5 URA3* CEN ARS]) (36). Strains with deletions of SAGA components or other factors were constructed by homologous recombination using PCR products of KAN-MX4 cassettes and G418 selection. Plasmids of *prp5*, *prp28, spt8, gcn5* and *ACT1-CUP1* reporter mutants were prepared by either in vivo gap repair cloning or traditional cloning.

Screen for suppressors of *prp5-GAR* cold-sensitivity

yYZX-02 cells (0.02 OD_{600}) carrying the cold-sensitive *prp5-GAR* allele were spread on 10 cm -Trp plates and grown overnight at 30°C. To generate random mutations, cell plates were irradiated with 10, 25 or 50 mJ/cm^2 ultraviolet light (Stratalinker, 254 nm) and then incubated at 16°C until colonies appeared (∼2 weeks). Suppressor colonies were then patched and cultured at 30°C. To exclude *cus2* mutations, the *CUS2* gene in each colony was amplified and Sanger sequenced. The remaining suppressor colonies were then transformed with yeast cDNA library plasmids. Plasmids in the yeast strains that reverted to 16°C cold sensi-

tivity were isolated and sequenced to find suppressor candidates, which were further identified by sequencing of their chromosomal counterpart genes.

6-Azauracil and copper assays

Yeast strains were first grown overnight in synthetic complete (SC) media without indicated amino acid(s) depending on the plasmid back-bone. Cells were then diluted to OD 0.2 at 600 nm when the culture reached mid-log phase. For 6-azauracil (6-AU) assays, yeast cells in 10-fold serial dilutions were spotted on plates containing 75 μg/ml of 6-azauracil (Sigma-Aldrich) and cultured at various temperatures. Plates were photographed each day to monitor growth. Copper assays were carried out as described (36,45). Plates were scored by the maximum copper tolerance of strain growth after 4 days culture at 30°C.

Co-Immunoprecipitation, western blotting, and RT-PCR

To perform in vivo co-IP, Prp5p was tagged at the N-terminus with FLAG through overlapping PCR and cloning on pRS314-*TRP* plasmid, Spt8p was tagged at C-terminus with 3xHA on pRS313-*HIS* plasmid. Both plasmids were then transformed into a *spt8* strain (yYZX15 with WT *PRP5* on a *URA* plasmid), and transformants were further selected to lose the *URA* plasmid using 5-FOA plates. Tag-containing strains were grown into mid-log phase and harvested, and the cell pellets were washed once in TBS buffer and the cell lysates were prepared by glass beads using lysis buffer (50 mM Tris–HCl, pH 7.0, 0.1% Triton, 150 mM NaCl) with protease inhibitors. Cleared lysates were then tumbled with anti-HA beads (Invitrogen) for 4 h at 4°C, followed by washing three times using the lysis buffer. Bead-bound proteins were separated on SDS-PAGE gels and probed with anti-HA (Invitrogen) or anti-Flag (Sigma) antibodies.

Purification of 6xHis-tagged full-length and truncated Prp5p proteins was described previously (46). GST-tagged Spt8p and Spt3p were generated by cloning coding sequences of *SPT8* and *SPT3* into pGEX-4T-1 and expressed in *Escherichia coli* (Rosetta) for 20 h at 16°C with 1.0 mM IPTG followed by purification using glutathione-sepharose (GE) under standard conditions. All purified proteins were dialyzed and stored in buffer D (20 mM HEPES–KOH at pH 7.9, 0.2 mM EDTA, 100 mM KCl, 0.5 mM dithiothreitol, 1 mM phenylmethylsulfonylfluoride, 20% glycerol). For *in vitro* protein–protein interaction assays, Prp5p proteins (40 pmol) were incubated with Spt8p or Spt3p (10 pmol) in 500 μl binding buffer (20 mM Tris–Cl at pH 8.0, 150 mM NaCl, 1mM EDTA, 0.2% Triton X-100, 0.5 mM PMSF) for 4 h at 4°C with Ni-NTA agarose. Bead pellets were washed four times with wash buffer (50 mM Tris–Cl at pH 8.0, 140 mM NaCl, 1 mM EDTA, 0.1% Triton X-100) and then resuspended in 50 μl of 1× sample loading buffer for SDS-PAGE electrophoresis. Spt8p, Spt3p and Prp5p were detected by western blotting using anti-GST (Sigma) or anti-His (Sigma) monoclonal antibodies.

Total RNA was isolated from yeast strains grown under various conditions, and RT-PCR was then performed as described (36,47). All related primers are listed in Supplementary Table S2.

Chromatin immunoprecipitation and Hiseq-PE150 sequencing

Chromatin Immunoprecipitation (ChIP) was performed as described (17). Yeast strains were grown overnight from a starting culture and diluted in fresh medium to reach mid-log phase. Cells were then either shifted to 16°C for an additional 30 min culture, or added to 6-AU (final 75 μg/ml) for additional 1 h culture at 30°C. For cross-linking, cells were treated with 1% formaldehyde for 15 min and then quenched by addition of glycine to 125 mM. After centrifugation, cell pellets were washed with cold TBS and lysed by glass beads in FA lysis buffer (50 mM HEPES–KOH at pH 7.5, 150 mM NaCl, 1 mM EDTA, 1% Triton X-100, 0.1% Na deoxycholate, 0.1% SDS, 1 mM PMSF) containing protease inhibitors. Chromatin was sheared using a Diagenode Bioruptor. Immunoprecipitations were performed using anti-RNA Pol II antibody (8WG16; Covance MMS-126R), anti-HA-agarose beads (Sigma), and anti-Flag M2 Affinity Agarose (Sigma). Associated DNAs were then purified using a PCR clean-up kit (Axygen) and analyzed by QuantStudio Real-Time PCR (Thermo Fisher) and Hiseq-PE150 (Novogene). For Real-Time PCR, primers used are as described (30,48), and the PCR signals from the immunoprecipitated samples were normalized to input.

The standard framework of ChIP-seq was used from *nf-core/ChIP-seq* version 1.1.0 pipeline (49): reads were aligned to *S. cerevisiae* genome (version R64–1-1) using *BWA* version 0.7.17-r1188; reads that were marked as duplicates and mapped to multiple locations were removed by *Samtools* version 1.9; read counts per bin were normalized to one million mapped reads (RPM) by *deepTools* version 3.2.1; peak calling used *MACS2* version 2.1.2. We used *DESeq2* version 1.22.2 to make differential binding analysis of different IP samples. IP enrichment signals were calculated using ratio of RPM_{IP} and RPM_{input}. Then, *deepTools* was used to draw the different value coverage of IP enrichment signal from two IP samples in exons, introns and 200 bp regions before the TSS. The gene annotation was obtained from the NCBI database.

RESULTS

spt8 mutants rescue the *cs* phenotype of the *prp5-GAR* allele

To identify additional interactions with or functions of Prp5p, we performed a yeast genetic screen using UV irradiation-induced mutagenesis and searched for suppressors that rescued the *cs* phenotype of the *prp5-GAR* allele (Figure 1A), which has mutations in the Prp5p SAT motif, has severely reduced ATPase activity, and is defective in splicing of branch site (BS) region mutant introns—i.e. introns with reduced base-pairing to U2 snRNA (36). The WT background *S. cerevisiae* strain with *prp5-GAR* allele cannot grow at the non-permissive temperature 16°C (Figure 1B); however, in the genetic screen we obtained dozens of clones that could grow at 16°C after UV-irradiation.

It was known that deletion of *CUS2*, encoding a protein component of U2 snRNP and an assumed functional target of Prp5p, rescued growth defects of the *ts prp5–1* al-

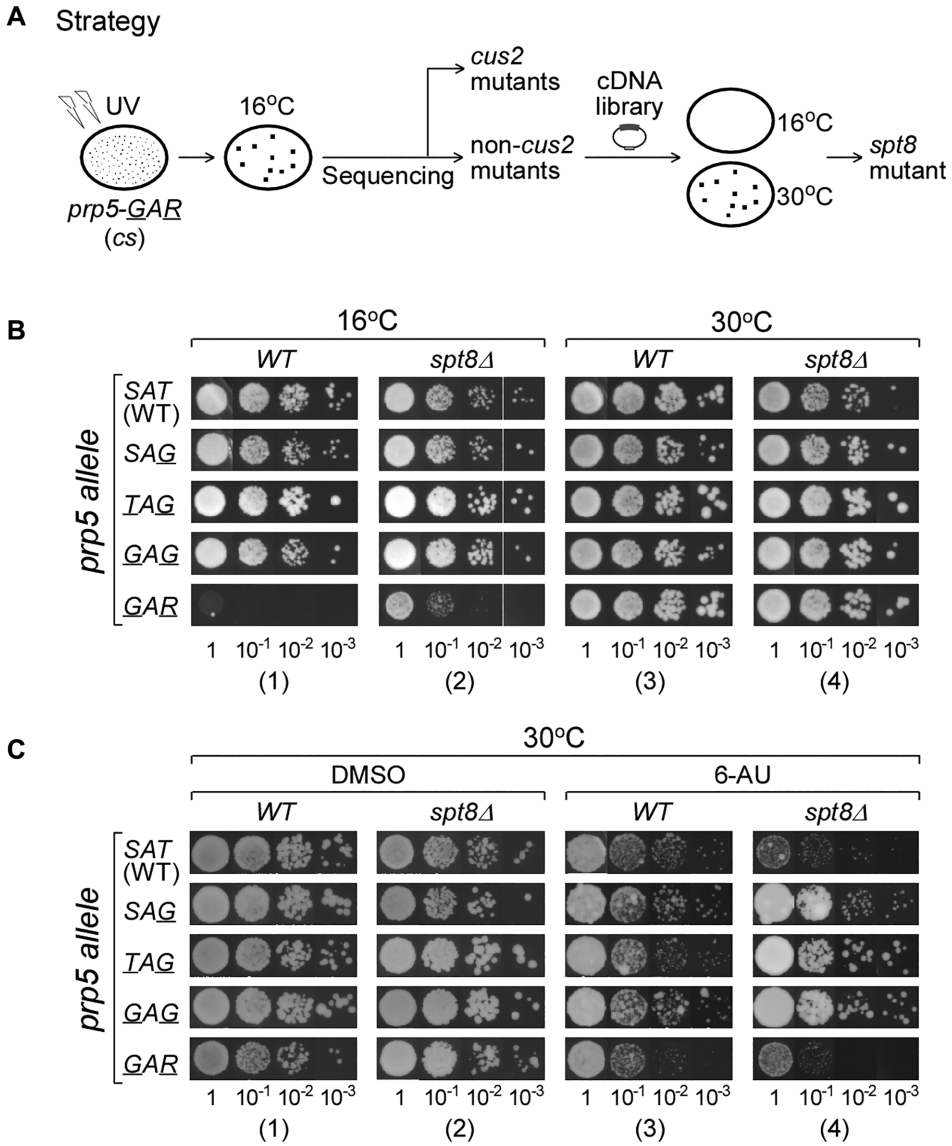

Figure 1. Reciprocal genetic interactions between transcription factor *SPT8* and splicing factor *PRP5*. (**A**) Strategy for genetic screen for suppressors of the cold sensitive (*cs*) *prp5-GAR* allele. One *spt8* mutant allele was obtained. (**B**) Deletion of *SPT8* gene rescues the *cs* phenotype of *prp5-GAR* allele at 16°C. (**C**) At the permissive temperature (30°C), *prp5* alleles (*-SAG*, *-TAG* and *-GAG*) rescue growth defects of *spt8Δ* allele on 6-AU.

lele (31,32) and of the *cs prp5-GAR* allele (36). To eliminate *cus2*-mutated clones, we first amplified and sequenced the *CUS2* gene in all suppressor clones, identifying more than 70% of clones that contained various mutations in *CUS2*, all of which introduced early stop codons thereby truncating Cus2p. We then focused on the non-*cus2*-mutated clones. We transformed cDNA library plasmids of *S. cerevisiae* (50) into the non-*cus2* suppressor-containing clones to search for plasmids that could restore the *cs* phenotype, and identified a library plasmid carrying full-length transcription factor *SPT8* that restored the yeast clone back to cold sensitivity. Further sequencing of this clone revealed that it had a mutation in the coding region of chromosomal *SPT8*, in which guanosine (position 980) was mutated to adenosine, introducing a stop codon (TAG) that terminated translation of Spt8p within its WD40 domain (Supplementary Figure S1A).

To confirm that loss of Spt8p, which is not essential for cell viability (51), suppressed *prp5-GAR* defects, we deleted the chromosomal *SPT8* gene (*spt8Δ*) in the *prp5-GAR* strain and validated that *spt8Δ* also rescued the *cs* phenotype of the *prp5-GAR* allele (Figure 1B, cf. columns 2 to 1). Deletion of *SPT8* did not change the growth of strains containing other *prp5-SAT* alleles (*-SAG*, *-TAG*, *-GAG*), all of which grew similarly to the WT *PRP5-SAT* strain at 16°C and 30°C (Figure 1B). Thus, inactivation of SAGA component Spt8p, either by mutation or deletion, partly rescues the severely ATPase-defective *prp5-GAR* allele.

prp5 alleles rescue growth defects due to *SPT8* deletion

Spt8p is a component of SAGA, a chromatin-modifying complex that contains two distinct enzymatic activities, acetylation and deubiquitination of histone residues, and

is involved in transcription initiation and elongation (27,28,52). We surmised from the *SPT8–PRP5* genetic interaction that *prp5* alleles might have previously-undetected effects on transcription. To address this possibility, we assayed growth in the presence of 6-azauracil (6-AU), which exacerbates transcription defects through inhibition of IMPDH, an enzyme catalyzing the first committed step in GMP biosynthesis (53,54). A series of *prp5* alleles, including *prp5-SAG*, *-TAG*, *-GAG* and *-GAR* that have decreased ATPase activities (51%, 42%, 22% and 4%, respectively, relative to WT PRP5-SAT, 36), were tested at the permissive temperature (30°C). In comparison to the WT *PRP5-SAT* allele, strains with *prp5-GAR* allele grew mildly worse on 6-AU, but other *prp5* mutant alleles did not show obvious defects in growth (Figure 1C, column 3). Consistent with Spt8p's primary function in transcription, growth of the *spt8Δ* strain on 6-AU was significantly inhibited (55); however, this inhibition was rescued by the presence of *prp5-SAG*, *-TAG* or *-GAG* alleles (Figure 1C column 4).

We further tested the 6-AU sensitivity at two other temperatures, 16°C and 37°C. At 16°C, all the yeast strains grew slower on 6-AU medium, but their patterns of inhibition and rescue were similar to that described above at 30°C (Supplementary Figure S1B). In contrast, at 37°C, the pattern was reversed: in the presence of all tested *prp5* alleles, cells grown on 6-AU were significantly inhibited; however, *spt8Δ* rescued growth on 6-AU of the WT *PRP5-SAT* and *prp5-GAR* alleles, but not *-SAG*, *-TAG*, or *-GAG* alleles (Supplementary Figure S1C). Taken together, these data suggest a reciprocal genetic interaction between Prp5p and Spt8p that impacts transcriptional elongation.

SPT3, another SAGA component, also genetically interacts with *PRP5*

The yeast SAGA complex is composed of 19 protein components, which are roughly divided into four modules according to their functions, TBP-binding (Spt8p and Spt3p), core structural (Ada1p, Spt7p, Spt20p, Taf5p, Taf6p, Taf9p, Taf10p, and Taf12p), deubiquitinating (Sgf11p, Sgf73p, Sus1p and Ubp8p), and HAT (Ada2p, Ada3p, and Gcn5p) (37,56,57). To address whether other components of the SAGA complex are also involved in a reciprocal genetic interaction with Prp5p, we further tested deletion of the *SPT3* gene, the other component of the TBP-binding module, and deletion of two genes selected from each of the other three SAGA modules, including *spt7Δ*, *spt20Δ*, *ubp8Δ*, *sgf11Δ*, *gcn5Δ* and *ada2Δ* (Figure 2A). None of the tested deletions could rescue the *cs* phenotype of *prp5-GAR* allele except for *spt3Δ*, which allowed yeast with *prp5-GAR* allele to grow at 16°C (Figure 2B, column 2), similar to the above findings with *spt8Δ*; in addition, the *spt3Δ* yeast strain grew slowly at 30°C, which was partially rescued by *prp5-GAR* allele (Figure 2B, cf. columns 4 to 3). Similarly, inhibition of growth on 6-AU of the *spt3Δ* strain could be rescued by *prp5-TAG* and *-GAG* alleles, but not by the *prp5-GAR* allele (Figure 2C, column 2). We note that *prp5-GAR* mildly reduces the growth at 30°C in the background of *spt7Δ and gcn5Δ* (Figure 2B, cf. columns 4 to 3).

GCN5 has genetic interactions with U2 snRNP protein component genes *LEA1/U2A′* and *MSL1/U2B″*, and *gcn5Δ* rescues the lethality of *LEA1* and *MSL1* double deletion (26). Therefore, we further used two *gcn5* mutant alleles, *gcn5-AAA*(KQL), which eliminates the HAT activity of Gcn5p, and *gcn5-AAA*(RGY), which retains intermediate HAT function (26), and tested their genetic interaction with *prp5* alleles. As with *gcn5Δ* above, these two *gcn5* mutant alleles could not rescue the *cs* phenotype of *prp5-GAR* allele (Supplementary Figure S2), indicating no detectable genetic interaction between *GCN5* and *PRP5* under the conditions tested here.

Therefore, these data reveal a previously unknown reciprocal genetic interaction between the TBP-binding module (*SPT8* and *SPT3*) of the SAGA complex and the spliceosomal ATPase gene *PRP5*. In one direction, *spt8Δ* or *spt3Δ* rescues the *cs* phenotype of the *prp5-GAR* allele, indicating that impaired splicing can be improved by deletion of transcription factors; in the other direction, *prp5* mutant alleles rescue the growth defects on 6-AU of *spt8Δ* and *spt3Δ*, indicating that impaired transcription can be improved by the slower spliceosomal ATPase.

Decreased RNA Pol II binding in the presence of *prp5* mutant alleles is reversed by *spt8Δ*

To further explore the mechanism of this genetic interaction between *PRP5* and *SPT8*/*SPT3*, we performed ChIP using Rbp1p antibody (8WG16) to detect occupancy of RNA Polymerase II (Pol II) on regions of two frequently tested genes: *DBP2*, an intron-containing gene, and *PDR5*, an intronless gene (48). At the permissive temperature (30°C), binding of Pol II on the intron-containing gene *DBP2* in the presence of *prp5-TAG* or *-GAR* allele was decreased across gene regions in comparison to the WT *PRP5-SAT* allele (Figure 3A upper left). Deletion of *SPT8* significantly decreased Pol II binding in the presence of all *prp5* alleles (Figure 3A upper right). After shift to the non-permissive temperature (16°C), binding of Pol II on *DBP2* was generally reduced and the inhibition by *prp5-TAG* allele was not as strong as at 30°C (Figure 3A lower left). In contrast, *spt8Δ* significantly improved Pol II binding on *DBP2* in the presence of *prp5-GAR* allele at 16°C, with a >4-fold enhancement on the promoter region in the presence of *prp5-GAR* allele compared to WT-*PRP5* (Figure 3A, lower right). However, on the intronless gene *PDR5*, we did not observe decreased Pol II binding in the presence of *prp5* mutant alleles, or the reverse effects by *spt8Δ* (Figure 3A′). Taken together, these results demonstrate that rescue of the *prp5-GAR cs* phenotype by *spt8Δ* correlates with the increased binding of RNA Pol II in an intron-dependent manner.

We next performed the same ChIP assays on yeast that grew in media with 6-AU, and found that 6-AU dramatically inhibited the binding of Pol II on both *DBP2* and *PDR5* genes (Supplementary Figure S3), as previously described (58). Similar to the above data (Figure 3A, lower right), in the presence of 6-AU, mutant *prp5* alleles inhibit Pol II binding on intron-containing gene *DBP2*, whereas *spt8Δ* allows slow *prp5* alleles to increase Pol II binding. These results are consistent with our genetic results (Figure 1), that *prp5-TAG* allele rescues cell growth on 6-AU when *SPT8* is deleted.

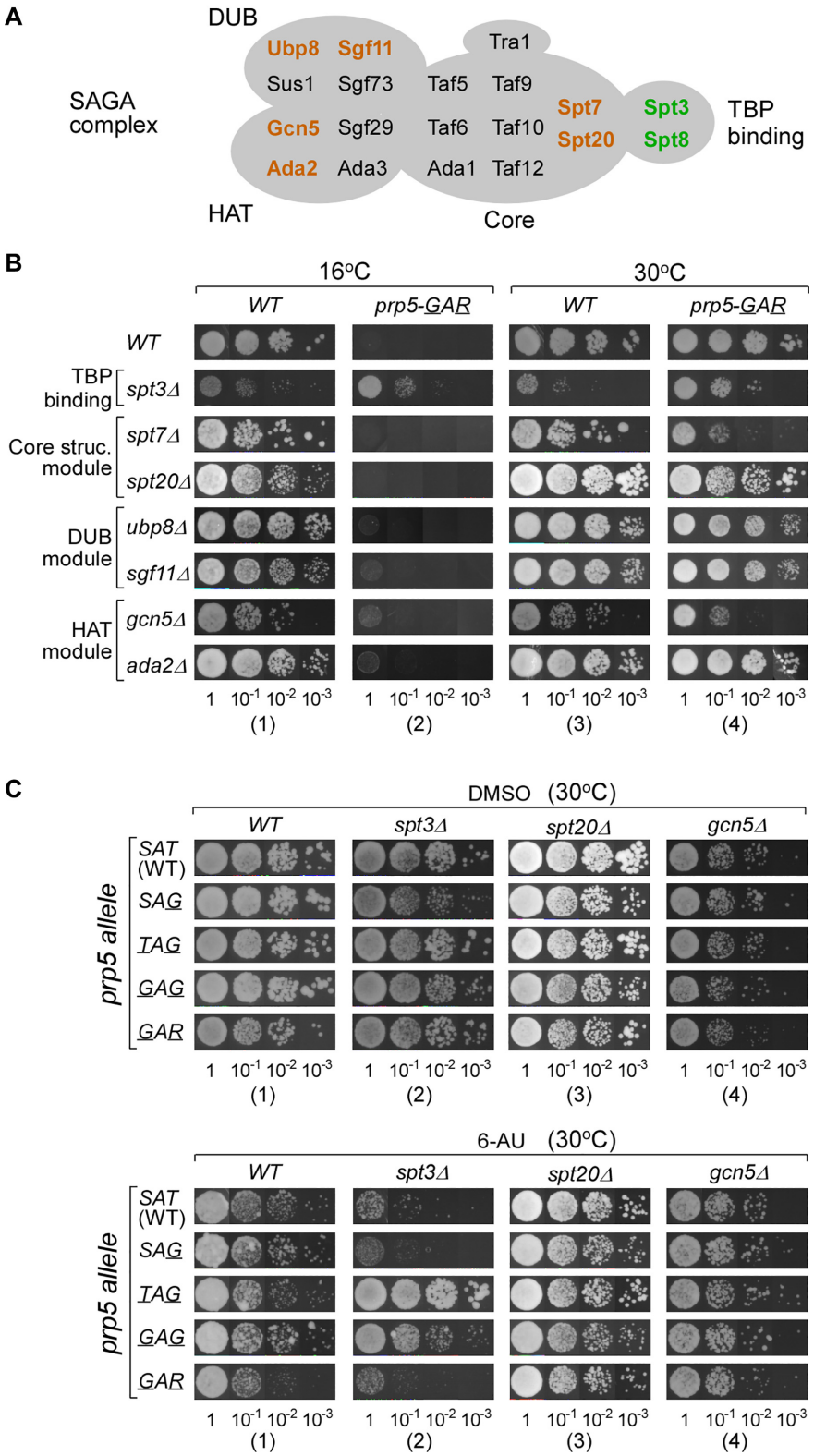

Figure 2. *SPT3*, another SAGA component, also genetically interacts with *PRP5*. (**A**) Illustration of the yeast SAGA complex. Components are classified into four groups (57), in which colored factors are tested in this study. (**B**) Deletion of *SPT3* rescues the *cs* phenotype of the *prp5-GAR* allele, whereas deletion of other tested SAGA components cannot. (**C**) *prp5* alleles (-*TAG* and -*GAG*) rescue growth defects of the *spt3Δ* allele on 6-AU.

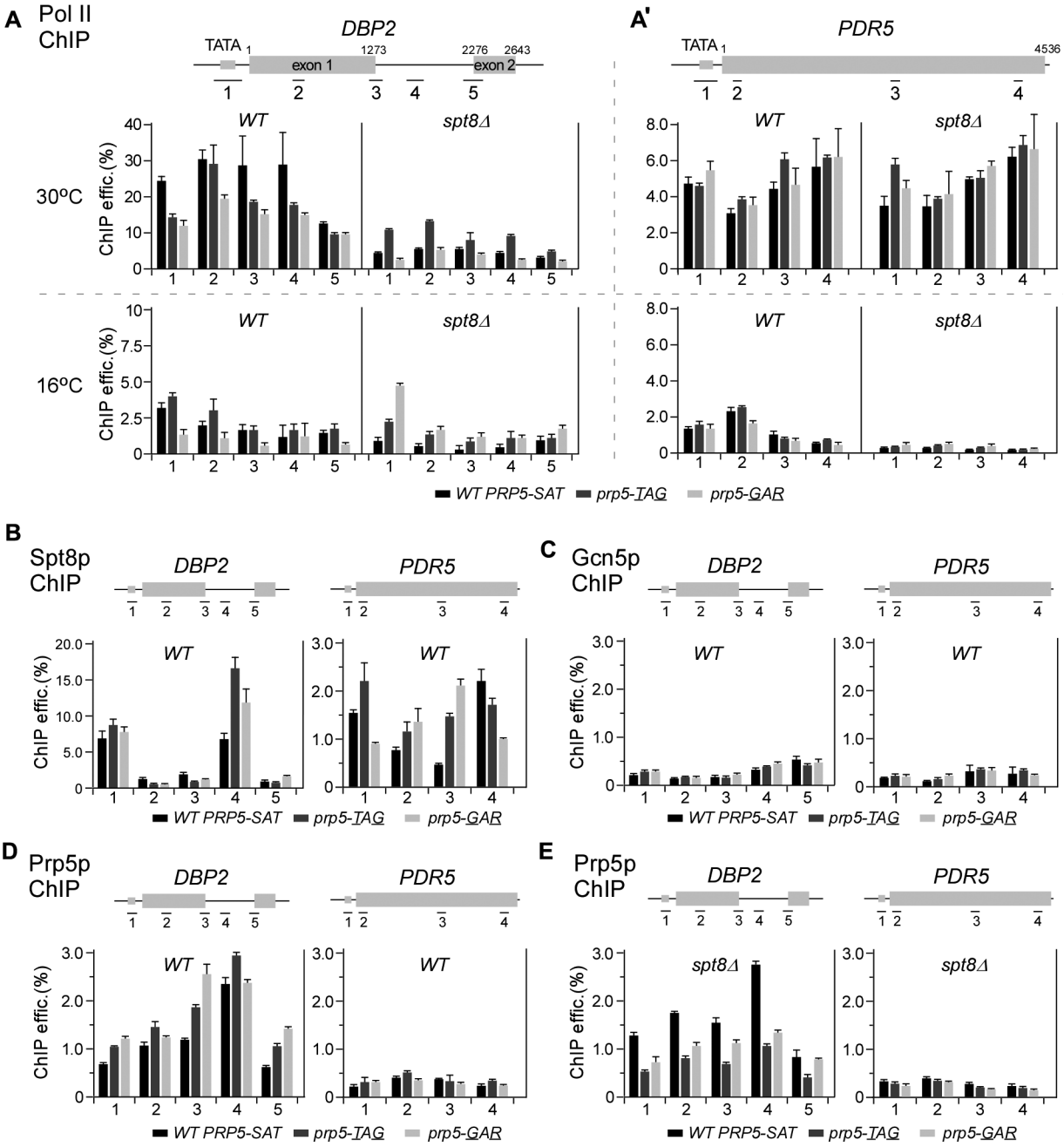

Figure 3. In the absence of *SPT8*, *prp5* mutant alleles stimulate RNA polymerase II binding to an intron-containing gene. ChIP assays on intron-containing gene *DBP2* and intronless gene *PDR5* were performed using RNA Pol II antibody 8WG16 (**A** and A'), anti-HA agarose for the HA-tagged Spt8 strain (**B**) and for the HA-tagged Gcn5 strain (**C**), and anti-Flag agarose for the Flag-tagged Prp5 strains with WT *SPT8* (**D**) or *spt8Δ* (**E**). Temperatures for yeast cultures and location of PCR primers are indicated. Bar graphs represent the co-immunoprecipitated signals and were normalized to input. All the data were analyzed from triplicates. Error bars represent standard deviation from the mean.

Spt8p and Prp5p reciprocally affect each other's recruitment to transcribed genes

To further address the role of Spt8–Prp5 interaction, we performed additional ChIP assays using antibodies against epitope tags on Spt8p, Gcn5p, and Prp5p (Figure 3B–E). First, we observed that Spt8p binds to promoter regions of both the intron-containing gene *DBP2* and the intronless gene *PDR5*; this binding was decreased after the transcription initiation site and then restored at the elongation stage, as previously described (59). In comparison to *WT PRP5-SAT*, *prp5-TAG*, and *-GAR* mutant alleles significantly enhanced the binding of Spt8p at the elongation stage (Figure 3B). Second, Gcn5p, a component of the HAT module, exhibited overall less binding and no obvious changes during transcription on both intron-containing and intronless genes; and the *prp5* alleles did not alter binding of Gcn5p (Figure 3C). These data again suggested that the function of Gcn5p is not coupled with Prp5p's activity. Third, we per-

formed Prp5p ChIP in yeast strains with or without *SPT8*. In the presence of *SPT8*, recruitment of WT Prp5p to the intron-containing gene *DBP2* was steadily increased from the transcription initiation site to the elongation stage, and *prp5* mutant proteins exhibited enhanced recruitment to *DBP2* (Figure 3D). In contrast, *spt8Δ* significantly changed the recruitment of Prp5p on *DBP2*: WT Prp5p was increased, whereas Prp5p mutants were significantly inhibited (cf. Figure 3D to E). However, for the intronless gene *PDR5*, recruitment of WT Prp5p and its mutants was not changed across the transcribed regions, and *spt8Δ* had no detectable effects (Figure 3D and E).

Taken together, these data demonstrate that slow *prp5* mutants enhance the recruitment of Spt8p to transcribing genes, especially at the elongation stage, and the presence of Spt8p facilitates the recruitment of Prp5p to the transcribing intron-containing gene. These results are globally consistent with the above-identified reciprocal genetic interactions.

Inhibited splicing caused by *prp5-GAR* is rescued by *SPT8* deletion

We previously found that *prp5-GAR* significantly inhibited splicing of the *WT ACT1-CUP1* reporter (36). Here, we investigated splicing changes of endogenous genes in the mutant strains by RT-PCR. In comparison to the *WT* strain, splicing of all eight tested intron-containing genes was inhibited in the *prp5-GAR* strain, exhibiting increased levels of pre-mRNA, but not in the *spt8Δ* strain (Figure 4A). Although the *prp5-GAR* allele is *cs*, splicing inhibition was already obvious at 30°C. Interestingly, the inhibited splicing caused by *prp5-GAR* was rescued by the *spt8Δ*, evidenced by a decrease of pre-mRNA level to a similar level as in the WT strain (Figure 4A). These data demonstrate that Spt8p contributes to the modulation of spliceosome assembly at the stage of U2 snRNP binding that is facilitated by the ATPase/RNA helicase Prp5p.

Genome-wide analysis of RNA Pol II binding shows that *prp5* mutation and *spt8Δ* globally rescue each other's effects

To further investigate the role of Prp5p–Spt8p interaction on genome-wide transcription, we performed ChIP-seq of yeast strains with *spt8Δ, prp5-GAR*, and both mutant alleles using the RNA Pol II antibody. At the permissive temperature, deletion of *SPT8* resulted in significantly decreased RNA Pol II binding over 661 genes (568 intronless genes plus 93 intron-containing genes), while 459 genes (442 plus 17) showed relatively mild increased Pol II binding (Figure 4B, left), consistent with the function of Spt8p being to facilitate transcription of a subset genes (60,61). The *prp5-GAR* allele decreased RNA Pol II binding over 327 genes (249 plus 78) and increased Pol II binding over 455 genes (438 plus 17), but with no significant direction preference as was observed for *spt8Δ* (Figure 4B middle). Interestingly, in the double mutant strain (*prp5-GAR*, *spt8Δ*), only 2 (decreased) and 132 (increased) genes showed significantly changed Pol II binding, suggesting a transcriptional effect of mutual rescue between the *prp5* mutation and *spt8Δ* (Figure 4B, right). In contrast, we did not observe this mutual rescue effect at the non-permissive temperature, because the *prp5-GAR* allele changed RNA Pol II binding of far fewer genes at 16°C (Figure 4B′).

To further address co-transcriptional splicing, we looked at the transcription profile of all intron-containing genes, and found that three of them had restored pausing of RNA Pol II in their intron regions in the double-mutant strain. For example, the well-studied co-transcriptional splicing gene, *DBP2*, has a high peak of RNA Pol II binding in the intronic region after the 5′SS in the WT strain, and this peak was decreased in the *prp5-GAR* strain but significantly restored with additional *spt8Δ*, especially at the 16°C (Figure 4C). A similar pattern was also found for two other intron-containing genes, *NOG2* and *RPL6B*, but most intron-containing genes did not exhibit an obvious pause of RNA Pol II around the intron region.

Prp5p physically interacts with Spt8p, but not with Spt3p

One possible basis of the Spt8p and Spt3p specific genetic interactions with Prp5p could be direct and physical interactions between the transcription and splicing factors. To address this, we first generated yeast strains in which Spt8p was tagged with 3xHA at its C-terminus and/or Prp5p was tagged with FLAG at its N-terminus; these tags did not change the *cs* phenotype of *prp5-GAR* allele (Supplementary Figure S4A). We found that Prp5p was co-immunoprecipitated with Spt8p using HA antibody in lysate from the double-tagged yeast strain, whereas no signal was detectable from the single-tagged yeast strain (Figure 5A, cf. lanes 4 to 3), suggesting that Spt8p and Prp5p form a stable interaction *in vivo*. Second, we tested *in vitro* protein-protein interactions using purified recombinant proteins and Ni-NTA beads, in which Prp5p was fused with a 6xHis tag, and Spt8p and Spt3p were fused to a GST tag. Pull-down assays showed that Prp5p directly interacted with Spt8p, but not Spt3p (Figure 5B). Furthermore, we also investigated the region of Prp5p required to interact with Spt8p. In contrast to the full-length Prp5p, two truncated Prp5p proteins without its N-terminal region (aa 1–206), ΔN and ΔN&ΔC, could not pull-down Spt8p. However, truncated Prp5p that lacked the C-terminal region, ΔC, still efficiently pulled-down Spt8p (Figure 5C). Although we were unable to express and test the N-terminal domain directly, these results imply that the N-terminal region of Prp5p is required for interaction with Spt8p.

We previously found that the N-terminal region of Prp5p also directly interacts with two different HEAT motif regions of Hsh155p/SF3B1, a U2 snRNP component (46). To address whether the Prp5p interaction with Spt8p and Hsh155p are mutually exclusive, an in vitro competition assay was performed. We found that Prp5p pulled down similar levels of Spt8p in the presence or absence of excess amounts of HEAT-motif fragments of Hsh155p (Supplementary Figure S4B), indicating that these two interactions might not be mutually exclusive. In addition, pull-down assays using yeast lysates showed that Spt8p-3HA could not co-IP Hsh155p (Supplementary Figure S4C). Taken together, these results suggest that Prp5p has different functional motifs within its N-terminal domain for these two interactions, but that the Prp5p-Spt8p and the

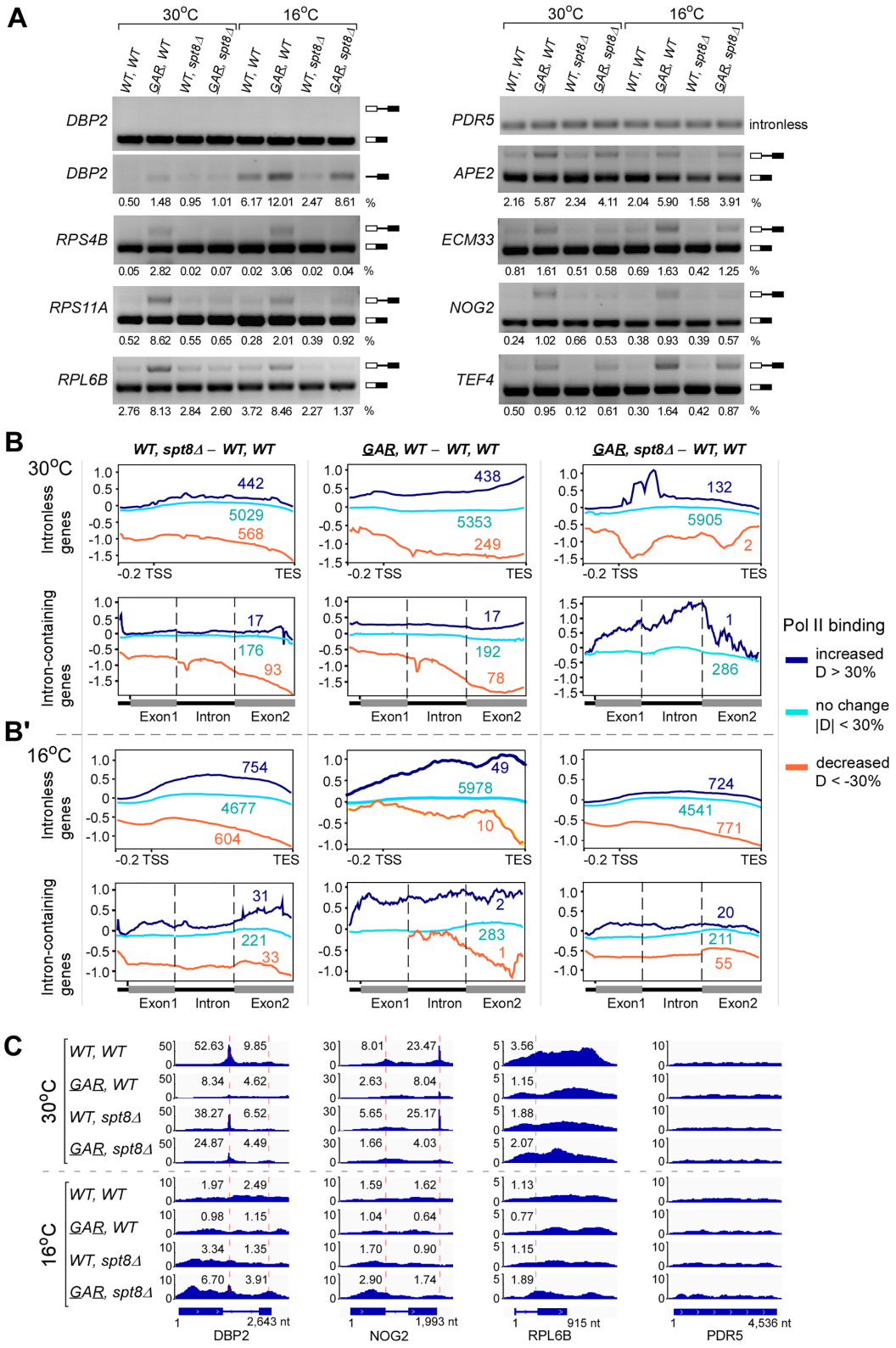

Figure 4. ChIP-seq reveals that global RNA Pol II binding is mutually rescued by *prp5-GAR* and *spt8Δ*. (**A**) Inhibited splicing by the *prp5-GAR* allele is restored by *SPT8* deletion. RT-PCRs were performed and the inhibited splicing ratios were semi-quantitated by signals of pre-mRNA / (pre-mRNA + mRNA) from triplicates. Analyses of genome-wide RNA Pol II binding on yeast genes in the presence of *prp5-GAR*, *spt8Δ*, and the double-mutant alleles at 30°C (**B**) and 16°C (**B'**). Intronless and intron-containing genes were separately analyzed, and genes were grouped into increased, no change and decreased RNA Pol II binding according to the total mapped reads that are normalized by input. Individual analyses of three genes with RNA Pol II pausing in the intronic regions suggested the restored pausing in the double-mutant strain (**C**).

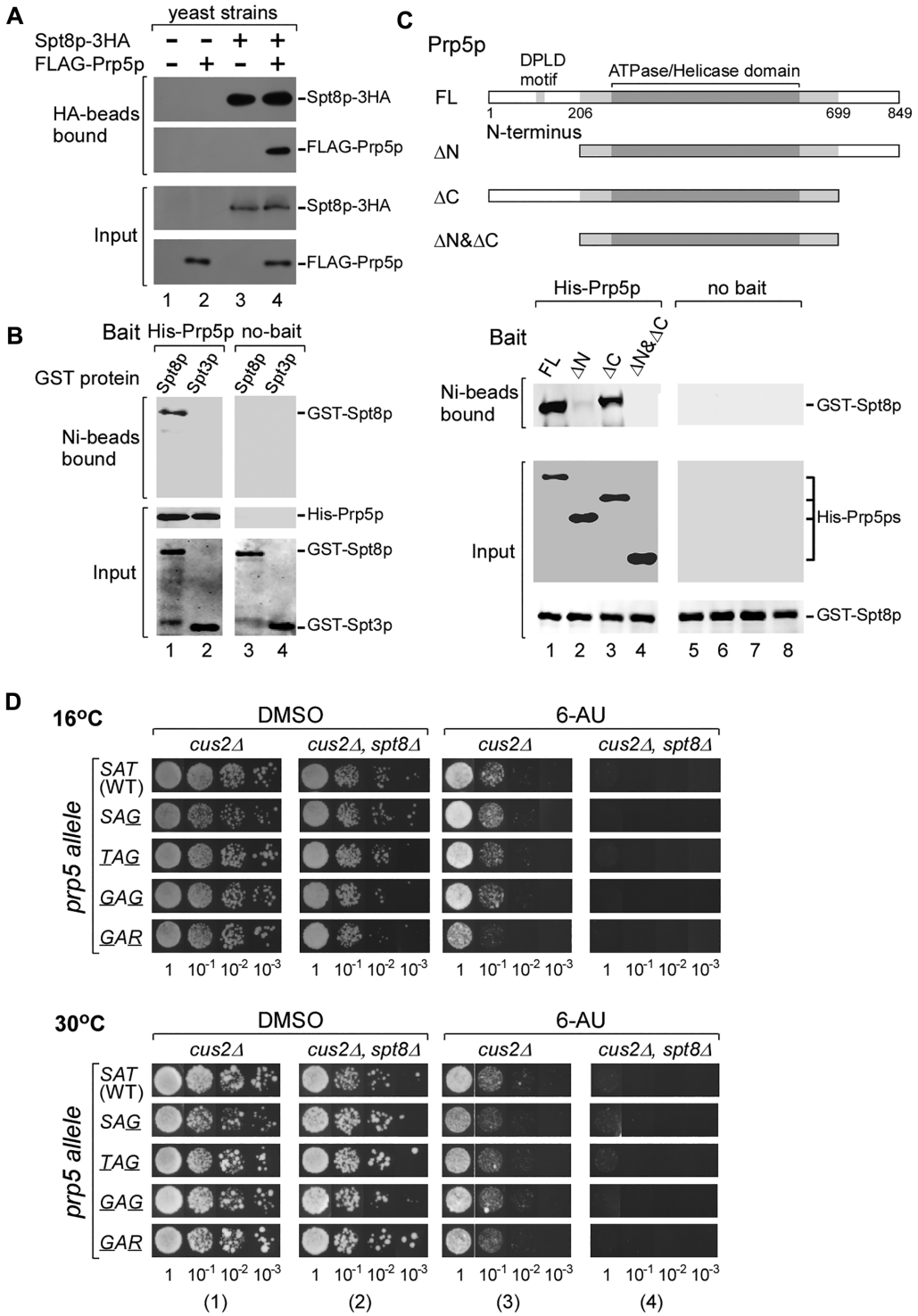

Figure 5. Prp5p physically interacts with Spt8p, but not Spt3p, in vivo and in vitro. (**A**) Spt8p interacts with Prp5p in cell lysate. In the cell lysate from a double-tagged strain, Spt8p-HA pulls down FLAG-Prp5p. Single-tagged strains are used as controls. (**B**) Prp5p directly interacts with Spt8p, but not Spt3p. Direct *in vitro* protein-protein interactions were tested using purified recombinant proteins and Ni-NTA agarose. Spt8p and Spt3p were GST-tagged, and Prp5p was fused to a 6xHis tag. No-bait pulldowns (i.e. beads alone) were used as controls. (**C**) The N-terminus of Prp5p is required for Spt8p–Prp5p interaction. *Upper*, schematic representation of the full-length and truncated Prp5p proteins. *Lower*, in vitro protein-protein interactions were tested as in panel B. (**D**) *CUS2* is required for maintaining the genetic interaction between *PRP5* and *SPT8*. *cus2Δ* abrogates the ability of all tested *prp5* alleles to rescue the growth defects of *spt8Δ* on 6-AU medium at 16°C and 30°C.

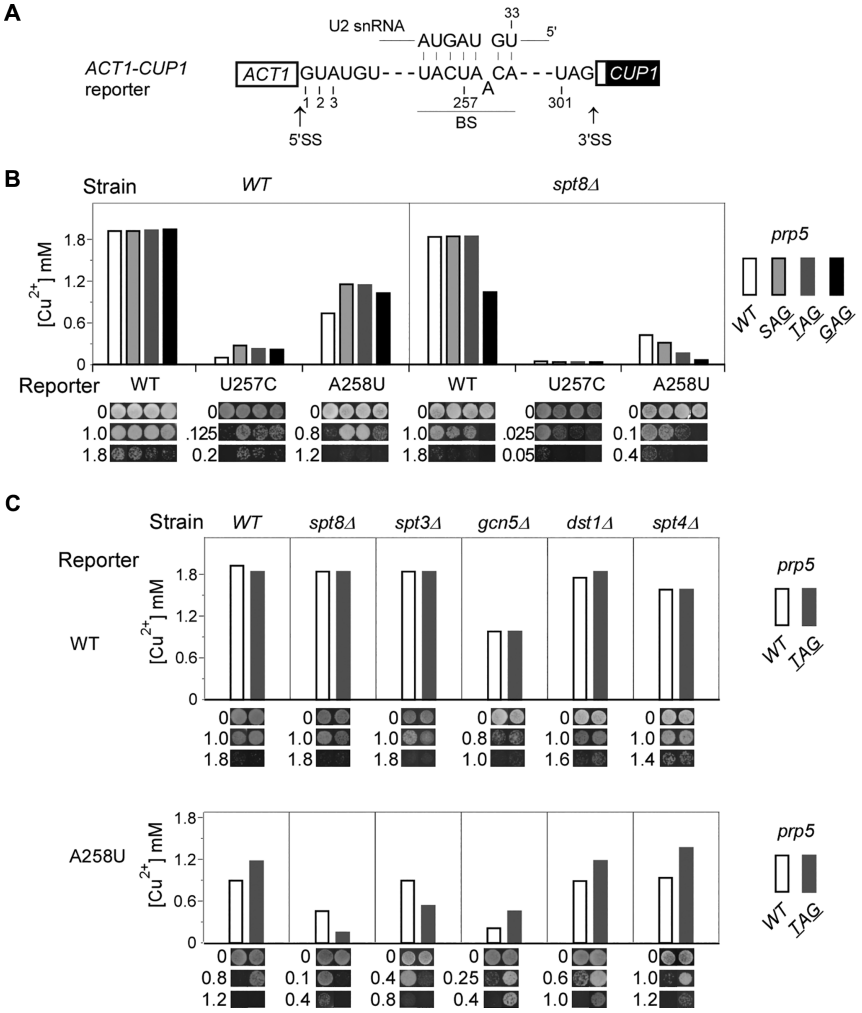

Figure 6. Deletion of the TBP-binding module components of SAGA complex, *SPT8* or *SPT3*, reverses *PRP5*-dependent proofreading at branch site region. (**A**) Schematic of the *ACT1-CUP1* reporter used for copper tolerance assay to monitor the efficiency of in vivo splicing. Mutant sites used in this study are indicated in red. (**B**) Deletion of *SPT8* reverses the improvement of splicing activity of suboptimal branch site region substrates by *prp5* alleles (SAT mutants). Growth of each strain on three representative copper concentrations was selected to illustrate altered splicing activities. (**C**) Deletion of *SPT3*, but not other transcription factors, also reverses proofreading at the branch site region by *PRP5*.

Prp5p-Hsh155p interactions are for the most part at different stages/times. However, this does not rule out the possibility of transient simultaneous interactions (see Discussion).

As mentioned previously, another critical splicing factor for the function of Prp5p is Cus2p, which binds to Hsh155p through a UHM-ULM interaction (62). Depletion of Cus2p allows U2-intron binding in vitro in the absence of ATP, although Prp5p is still physically required (31,63,64); in vivo, *cus2Δ* suppresses a transcriptional elongation defect wherein RNA Pol II accumulates on introns (30). To address the role of *CUS2* in the Prp5p−Spt8p interaction, we performed 6-AU assays in the *cus2Δ* background. In the absence of *CUS2*, the *prp5-GAR* allele is no longer *cs* (Figure 5D upper), as previously described (36). Deletion of *CUS2* resulted in sensitivity to 6-AU and abrogated the rescue of *spt8Δ* growth defects on 6-AU by *prp5* alleles under all tested temperatures (Figure 5D and Supplementary Figure S5A). Thus, *CUS2* is required for maintaining the Spt8p−Prp5p interaction-mediated coupling between transcription and splicing.

SPT8 and *SPT3* contribute to BS proofreading by *PRP5*

Prp5p alleles, depending on their relative ATPase activities, can modulate the use of weak BS:U2 snRNA duplexes in splicing (36,47,65). We addressed whether disrupting the above-identified interactions would alter the BS region selectivity using the well-characterized splicing reporter gene *ACT1-CUP1* in *S. cerevisiae* (45), where the tolerance to copper in the media is proportional to the splicing of the reporter intron (Figure 6A). In the WT *SPT8* background, *prp5-SAG*, *-TAG* and *-GAG* alleles that are slow ATPases relative to WT *PRP5-SAT* improved splicing of suboptimal BS region substrates, such as U257C and A258U, whereas the WT reporter was unchanged, as previously reported (Figure 6B, left; 36). However, in the absence of *SPT8*, *prp5-SAT* mutant alleles no longer improved splicing of subop-

timal BS substrates; instead, their splicing activities were decreased (Figure 6B, right); *spt3Δ* showed the same loss of improved splicing due to slow-ATPase *prp5* alleles (Figure 6C). In contrast, deletion of other transcription factors, such as *GCN5*, *DST1*, or *SPT4*, did not alter the improved splicing of suboptimal BS substrate by SAT motif mutant allele *prp5-TAG* (Figure 6C). The exacerbation of BS region mutants in the absence of *SPT8* is likely due to the failure of *prp5* mutants to be recruited. These results indicate that the Prp5–Spt8/Spt3 interaction modulates splicing proofreading at the BS region.

DISCUSSION

Prp5p is an RNA-dependent ATPase required for early spliceosome assembly and has been proposed to contribute to a splicing-dependent transcriptional checkpoint associated with pre-spliceosome formation (U1–U2–intron complexes) (30). In this study, we find partner proteins for Prp5p's coupling to the transcriptional machinery in the TBP-binding module of the SAGA complex. This is supported by several lines of evidence: (i) reciprocal genetic interactions between *PRP5* and SAGA components, limited to *SPT8* and *SPT3*; (ii) direct physical interaction between Prp5p and Spt8p; (iii) contribution of Spt8p and Prp5p to each other's recruitment to transcribed genes; (iv) global restoration of affected transcription in the *prp5-GAR* and *spt8Δ* double-mutant strain; (v) inhibited splicing by a *prp5* mutant allele is rescued by *spt8Δ* and (vi) influence of Spt8p and Spt3p on Prp5p-dependent splicing proofreading at the BS region.

Reciprocal genetic interactions

Our data reveal a reciprocal genetic interaction between the TBP-binding module (*SPT8* and *SPT3*) of SAGA complex and the spliceosomal ATPase gene *PRP5*. In one direction, *spt8Δ* or *spt3Δ* rescues the *cs* phenotype of the *prp5-GAR* allele, indicating that impaired splicing can be improved by deletion of transcription factors; in the other direction, *prp5* mutant alleles with reduced ATPase activities rescue the growth defects on 6-AU of *spt8Δ* and *spt3Δ*, indicating that impaired transcription can be improved by the slower spliceosomal ATPase. This reciprocal relationship suggests that in WT cells there is a balance of activity of Prp5p and Spt8p/Spt3p. Mutation of either of these results in defects due to imbalance; in contrast, mutation of both restores this balance.

The genetic interaction of *PRP5* with both *SPT8* and *SPT3* is consistent with previous findings that *SPT8* and *SPT3* are functionally similar to each other, form the TBP-binding module (51,57,60), and are structurally separated from other SAGA components (27). Null mutations in *SPT8* are suppressed by several *spt3* mutations (51). Along with Spt3p, one proposed role of Spt8p is to control the TBP–TATA interaction at the promoter region, identified by chemical crosslinking (66).

Direct Prp5p–Spt8p interaction

The reciprocal genetic effects of *prp5* mutants and *spt8Δ*/*spt3Δ* suggested that they might be direct binding partners. We found that Prp5p and Spt8p co-immunoprecipitate from yeast lysates, indicating association within a complex. We directly tested this by making recombinant His-Prp5p, GST-Spt8p, and GST-Spt3p proteins and performed *in vitro* binding and pull-down assays (Figure 5). Prp5p directly interacts with Spt8p, but not Spt3p; this is consistent with newly revealed cryo-EM structures of the yeast SAGA complexes, in which Spt3p is located within the central core module (relatively inaccessible), while Spt8p is positioned outside on the adjacent surface (67,68).

Other described interactions between SAGA transcription components and splicing factors include U2 snRNP components, Lea1p/U2A′ and Msl1p/U2B", with *GCN5* in yeast (26), the co-purification of U2 snRNP SF3B3 (SAP130) with human GCN5-containing STAGA complex (41), and the co-purification of both U2 snRNP SF3B3 and SF3B5 with *Drosophila* SAGA (44). Recently, transcription elongation factor Spt5p has been shown to contribute to splicing efficiency by recruitment of U5 snRNP to intron-containing genes (69).

We previously demonstrated direct protein-protein interaction between Prp5p and Hsh155p, orthologue of human SF3B1 (46). Both Prp5p–Hsh155p and Prp5p–Spt8p interactions require the N-terminal domain of Prp5p, but we could not detect any mutual exclusivity of these interactions (Supplementary Figure S4). It is tempting to suggest that these interactions may occur simultaneously. This may help to first recruit Prp5p and U2 snRNPs to SAGA at the promoter of transcribed genes, and then subsequently to pass off Prp5p from SAGA to the Hsh155p component of U2 snRNP as U2 snRNA recognizes the branch site sequence in the transcript (Figure 7). Such simultaneous interaction would likely be transient, during pre-spliceosome formation itself, as pull-down assays using yeast lysates showed that Spt8p-3HA did not detectably co-IP Hsh155p. Further work is needed to address these possibilities.

Prp5p–Spt8p interaction guides proper transcription and splicing

The physical interaction between splicing factor Prp5p and SAGA component Spt8p is important for the coupling between transcription and splicing (Figure 7A). Spt8p and the TBP-binding module of SAGA recruit Prp5p to the promoter region. The Spt8p−Prp5p interaction ensures proper initiation and elongation of transcription by RNA Pol II (Figures 3 and 4) and modulation of splicing proofreading of intron-containing gene at the BS region by Prp5p (Figure 6). In the presence of the WT Prp5p, lack of Spt8p significantly alters transcription of a subset of both intronless and intron-containing genes, in which most are down-regulated, but does not change the splicing efficiency of intron-containing genes (Figure 7B). On the other hand, in the presence of Spt8p, *prp5* allele (*GAR*) also affects transcription of a subset of intronless and intron-containing genes and inhibits pre-mRNA splicing of the intron-containing genes (Figure 7C). However, the double-mutant (*prp5-GAR* and *spt8Δ*) restores the affected transcription and the inhibited pre-mRNA splicing (Figure 7D).

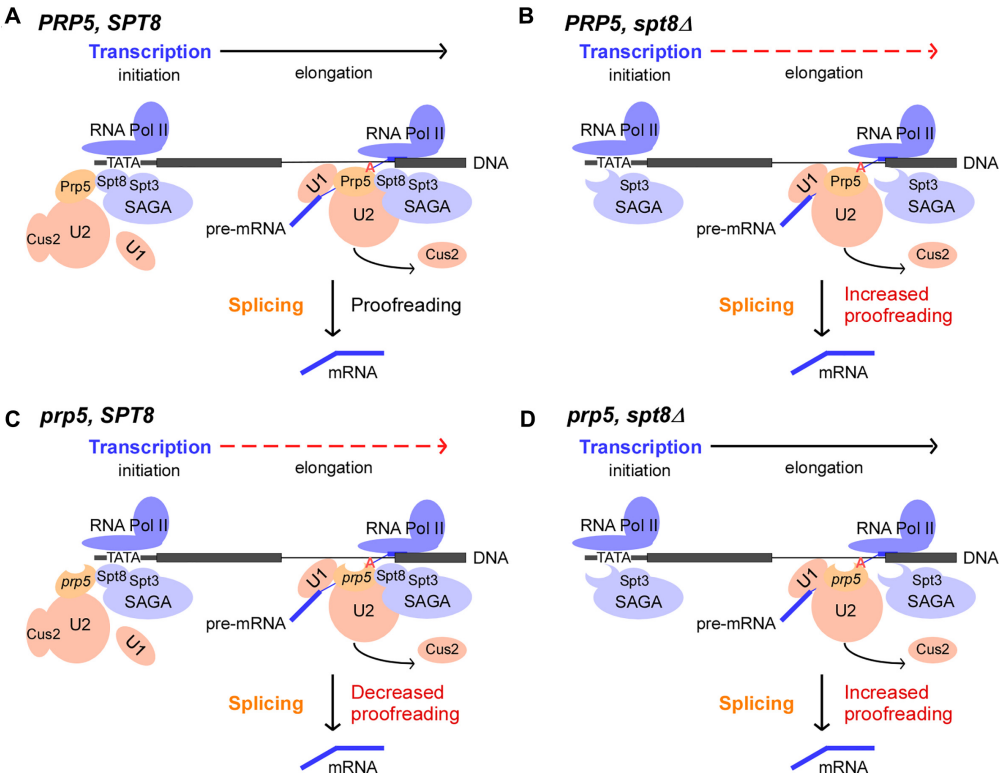

Figure 7. Coupling between transcription and splicing mediated by Spt8p/Spt3p and Prp5p. (**A**) Schematic depicting recruitment of Prp5p to the promoter region by the TBP-binding module of SAGA (Spt8p and Spt3p) and subsequent modulation of splicing proofreading at the BS region by Prp5p. This recruitment relies on direct interaction between Prp5p and Spt8p. (**B**) Deletion of *SPT8* results in altered transcription of a subset of intronless and intron-containing genes, most are down-regulated. Loss of *SPT8*/*SPT3* increases splicing proofreading at the BS region. (**C**) The *prp5* mutant allele affects transcription of a subset of intronless and intron-containing genes and inhibits pre-mRNA splicing. (**D**) The double mutant, *prp5* allele and deletion of *SPT8*, restores both affected transcription and inhibited pre-mRNA splicing. Cus2p plays a critical role in this coupling, deletion of *CUS2* abrogates the coupling between transcription and splicing. Lack of Spt8p/Spt3p results in increased splicing proofreading on suboptimal BS substrates. For clarity, intronless genes are not depicted.

The meaning of changes in BS fidelity

In the above model, Prp5p–Spt8p interaction promotes pre-spliceosome formation (Complex A). These findings lead us to propose that Prp5p–Spt8p interactions accelerate pre-spliceosome formation; this specifically suppresses splicing defects caused by suboptimal branch site region substrates. Conversely, loss of Prp5p–Spt8p interaction slows pre-spliceosome formation; this exacerbates splicing defects of suboptimal BS substrates (Figure 6). That a lack of Spt8p/Spt3p results in increased splicing proofreading on suboptimal BS substrates suggests that the Spt8p−Prp5p interaction contributes to both the efficiency of transcription and the fidelity of splicing. These data suggest that Spt8p/Spt3p have a direct effect on U2 snRNP function at the time of branch site recognition; alternatively, they may alter the quality (i.e. some feature) of U2 snRNPs that are recruited to nascent transcripts.

We note that the *prp5-GAR* mutant also changes the RNA Pol II occupancy on hundreds of intronless genes; this was unanticipated, suggesting that the recruitment of Prp5p to transcribed genes by Spt8p might not be intron- or splicing-dependent. Although the change in Pol II occupancy on intronless genes could be due to indirect effects, this possibility is less likely due to the short time interval (30 min) at the non-permissive temperature. The possible role of Prp5p on non-intron-containing genes will require further investigation.

As a splicing factor, deletion of *CUS2* causes strong growth defects on 6-AU (Figure 5D), suggesting that it has a critical role in yeast transcription, and this is consistent with previous reports (30,70). The homolog of the yeast Cus2p in humans is Tat-SF1 (29), first identified as a Tat-dependent elongation factor important for HIV transcription (71). Removal of Cus2p is a powerful suppressor of the defect of ATPase deficient mutant Prp5p proteins (72). In the absence of *CUS2*, the Prp5p-Spt8p interaction-mediated coupling is no longer detectable, indicating a dynamic relationship between the transcription subcomplex SAGA and the spliceosome subcomplex U2 snRNP, and its mechanism needs further investigation. It is intriguing that all three identified suppressors of mutant *prp5* (*CUS2, SPT8*, and *SPT3*) encode transcription factors, which underscores a role for Prp5p in mediating a connection between transcription and spliceosome assembly.

We considered the possibility that the Prp5p–Spt8p interaction represents non-canonical roles for these proteins. However, because *prp5* mutants alter Spt8p-dependent pol II occupancy, and *spt8Δ* alters the Prp5p-dependent use of sub-optimal branch site sequences, we conclude that the in-

teractions between Spt8p and Prp5p contribute to their respective canonical roles. We also performed 6-AU assays of *spt8Δ* with mutants of another ATPase Prp28p, which is required for a later stage of spliceosome assembly, facilitating the transition from 5'SS:U1 snRNA base-pairing to 5'SS:U6 snRNA base-pairing and resulting in the release of U1 snRNP (73,74). Using a series of *prp28* mutants *(-E404K*, *-E404V*, *-E404L*, *-E404A)* previously identified (75), we did not observe any detectable genetic interaction between *SPT8* and *PRP28* (Supplementary Figure S5). These data suggest that the effects on splicing of the interaction between Spt8p and splicing factors is limited to pre-spliceosome assembly.

DATA AVAILABILITY

All NGS data have been deposited to NCBI under accession number GSE147179.

SUPPLEMENTARY DATA

Supplementary Data are available at NAR Online.

FUNDING

National Natural Science Foundation of China [31400653, 31525022, 31472045, 31570821, 31971225]; National Institutes of Health [GM57829]; Hundred Talents program of Anhui Province [KJ2017A190], Scientific Research of BSKY [XJ201601]; Anhui Medical University Translational Medicine Program [2017ZHYX09]. Funding for open access charge: Scientific Research of BSKY from Anhui Medical University [XJ201601].
Conflict of interest statement. None declared.

REFERENCES

1. Darnell,J.E. Jr. (2013) Reflections on the history of pre-mRNA processing and highlights of current knowledge: a unified picture. *RNA*, **19**, 443–460.
2. Pai,A.A. and Luca,F. (2018) Environmental influences on RNA processing: Biochemical, molecular and genetic regulators of cellular response. *Wiley Interdiscip Rev. RNA*, **10**, e1503.
3. Alpert,T., Herzel,L. and Neugebauer,K.M. (2017) Perfect timing: splicing and transcription rates in living cells. *Wiley Interdiscip Rev. RNA*, **8**, e1401.
4. Saldi,T., Cortazar,M.A., Sheridan,R.M. and Bentley,D.L. (2016) Coupling of RNA polymerase II transcription elongation with pre-mRNA splicing. *J. Mol. Biol.*, **428**, 2623–2635.
5. Maniatis,T. and Reed,R. (2002) An extensive network of coupling among gene expression machines. *Nature*, **416**, 499–506.
6. Pandit,S., Wang,D. and Fu,X.D. (2008) Functional integration of transcriptional and RNA processing machineries. *Curr. Opin. Cell. Biol.*, **20**, 260–265.
7. Haberle,V. and Stark,A. (2018) Eukaryotic core promoters and the functional basis of transcription initiation. *Nat. Rev. Mol. Cell. Biol.*, **19**, 621–637.
8. Das,R., Yu,J., Zhang,Z., Gygi,M.P., Krainer,A.R., Gygi,S.P. and Reed,R. (2007) SR proteins function in coupling RNAP II transcription to pre-mRNA splicing. *Mol. Cell.*, **26**, 867–881.
9. de la Mata,M. and Kornblihtt,A.R. (2006) RNA polymerase II C-terminal domain mediates regulation of alternative splicing by SRp20. *Nat. Struct. Mol. Biol.*, **13**, 973–980.
10. Dye,M.J., Gromak,N. and Proudfoot,N.J. (2006) Exon tethering in transcription by RNA polymerase II. *Mol. Cell.*, **21**, 849–859.
11. Nojima,T., Rebelo,K., Gomes,T., Grosso,A.R., Proudfoot,N.J. and Carmo-Fonseca,M. (2018) RNA Polymerase II Phosphorylated on CTD Serine 5 Interacts with the Spliceosome during Co-transcriptional Splicing. *Mol. Cell.*, **72**, 369–379.
12. Lin,S., Coutinho-Mansfield,G., Wang,D., Pandit,S. and Fu,X.D. (2008) The splicing factor SC35 has an active role in transcriptional elongation. *Nat. Struct. Mol. Biol.*, **15**, 819–826.
13. Sapra,A.K., Anko,M.L., Grishina,I., Lorenz,M., Pabis,M., Poser,I., Rollins,J., Weiland,E.M. and Neugebauer,K.M. (2009) SR protein family members display diverse activities in the formation of nascent and mature mRNPs in vivo. *Mol. Cell.*, **34**, 179–190.
14. Fong,Y.W. and Zhou,Q. (2001) Stimulatory effect of splicing factors on transcriptional elongation. *Nature.*, **414**, 929–933.
15. Loerch,S., Leach,J.R., Horner,S.W., Maji,D., Jenkins,J.L., Pulvino,M.J. and Kielkopf,C.L. (2019) The pre-mRNA splicing and transcription factor Tat-SF1 is a functional partner of the spliceosome SF3b1 subunit via a U2AF homology motif interface. *J. Biol. Chem.*, **294**, 2892–2902.
16. David,C.J., Boyne,A.R., Millhouse,S.R. and Manley,J.L. (2011) The RNA polymerase II C-terminal domain promotes splicing activation through recruitment of a U2AF65-Prp19 complex. *Genes. Dev.*, **25**, 972–983.
17. Kress,T.L., Krogan,N.J. and Guthrie,C. (2008) A single SR-like protein, Npl3, promotes pre-mRNA splicing in budding yeast. *Mol. Cell.*, **32**, 727–734.
18. Wallace,E.W.J. and Beggs,J.D. (2017) Extremely fast and incredibly close: cotranscriptional splicing in budding yeast. *RNA*, **23**, 601–610.
19. de la Mata,M., Alonso,C.R., Kadener,S., Fededa,J.P., Blaustein,M., Pelisch,F., Cramer,P., Bentley,D. and Kornblihtt,A.R. (2003) A slow RNA polymerase II affects alternative splicing in vivo. *Mol. Cell.*, **12**, 525–532.
20. Dujardin,G., Lafaille,C., Petrillo,E., Buggiano,V., Gomez Acuna,L.I., Fiszbein,A., Godoy Herz,M.A., Nieto Moreno,N., Munoz,M.J., Allo,M. *et al.* (2013) Transcriptional elongation and alternative splicing. *Biochim. Biophys. Acta.*, **1829**, 134–140.
21. Fong,N., Kim,H., Zhou,Y., Ji,X., Qiu,J., Saldi,T., Diener,K., Jones,K., Fu,X.D. and Bentley,D.L. (2014) Pre-mRNA splicing is facilitated by an optimal RNA polymerase II elongation rate. *Genes. Dev.*, **28**, 2663–2676.
22. Bentley,D.L. (2014) Coupling mRNA processing with transcription in time and space. *Nat. Rev. Genet.*, **15**, 163–175.
23. Ji,X., Zhou,Y., Pandit,S., Huang,J., Li,H., Lin,C.Y., Xiao,R., Burge,C.B. and Fu,X.D. (2013) SR proteins collaborate with 7SK and promoter-associated nascent RNA to release paused polymerase. *Cell.*, **153**, 855–868.
24. Close,P., East,P., Dirac-Svejstrup,A.B., Hartmann,H., Heron,M., Maslen,S., Chariot,A., Soding,J., Skehel,M. and Svejstrup,J.Q. (2012) DBIRD complex integrates alternative mRNA splicing with RNA polymerase II transcript elongation. *Nature*, **484**, 386–389.
25. Batsche,E., Yaniv,M. and Muchardt,C. (2006) The human SWI/SNF subunit Brm is a regulator of alternative splicing. *Nat. Struct. Mol. Biol.*, **13**, 22–29.
26. Gunderson,F.Q. and Johnson,T.L. (2009) Acetylation by the transcriptional coactivator Gcn5 plays a novel role in co-transcriptional spliceosome assembly. *PLoS. Genet.*, **5**, e1000682.
27. Wu,P.Y., Ruhlmann,C., Winston,F. and Schultz,P. (2004) Molecular architecture of the S. cerevisiae SAGA complex. *Mol. Cell.*, **15**, 199–208.
28. Wu,P.Y. and Winston,F. (2002) Analysis of Spt7 function in the Saccharomyces cerevisiae SAGA coactivator complex. *Mol. Cell. Biol.*, **22**, 5367–5379.
29. Yan,D., Perriman,R., Igel,H., Howe,K.J., Neville,M. and Ares,M. Jr. (1998) CUS2, a yeast homolog of human Tat-SF1, rescues function of misfolded U2 through an unusual RNA recognition motif. *Mol. Cell Biol.*, **18**, 5000–5009.
30. Chathoth,K.T., Barrass,J.D., Webb,S. and Beggs,J.D. (2014) A splicing-dependent transcriptional checkpoint associated with prespliceosome formation. *Mol. Cell*, **53**, 779–790.
31. Perriman,R., Barta,I., Voeltz,G.K., Abelson,J. and Ares,M. Jr. (2003) ATP requirement for Prp5p function is determined by Cus2p and the structure of U2 small nuclear RNA. *Proc. Natl. Acad. Sci. U.S.A.*, **100**, 13857–13862.

32. Perriman,R.J. and Ares,M. Jr. (2007) Rearrangement of competing U2 RNA helices within the spliceosome promotes multiple steps in splicing. *Genes. Dev.*, **21**, 811–820.
33. Abu Dayyeh,B.K., Quan,T.K., Castro,M. and Ruby,S.W. (2002) Probing interactions between the U2 small nuclear ribonucleoprotein and the DEAD-box protein, Prp5. *J. Biol. Chem.*, **277**, 20221–20233.
34. Ruby,S.W., Chang,T.H. and Abelson,J. (1993) Four yeast spliceosomal proteins (PRP5, PRP9, PRP11, and PRP21) interact to promote U2 snRNP binding to pre-mRNA. *Genes. Dev.*, **7**, 1909–1925.
35. Xu,Y.Z., Newnham,C.M., Kameoka,S., Huang,T., Konarska,M.M. and Query,C.C. (2004) Prp5 bridges U1 and U2 snRNPs and enables stable U2 snRNP association with intron RNA. *EMBO. J.*, **23**, 376–385.
36. Xu,Y.Z. and Query,C.C. (2007) Competition between the ATPase Prp5 and branch region-U2 snRNA pairing modulates the fidelity of spliceosome assembly. *Mol. Cell.*, **28**, 838–849.
37. Rodriguez-Navarro,S. (2009) Insights into SAGA function during gene expression. *EMBO. Rep.*, **10**, 843–850.
38. Rodriguez-Navarro,S., Fischer,T., Luo,M.J., Antunez,O., Brettschneider,S., Lechner,J., Perez-Ortin,J.E., Reed,R. and Hurt,E. (2004) Sus1, a functional component of the SAGA histone acetylase complex and the nuclear pore-associated mRNA export machinery. *Cell*, **116**, 75–86.
39. Will,C.L. and Luhrmann,R. (2011) Spliceosome structure and function. *Cold Spring Harbor Perspect. Biol.*, **3**, a003707.
40. Brand,M., Moggs,J.G., Oulad-Abdelghani,M., Lejeune,F., Dilworth,F.J., Stevenin,J., Almouzni,G. and Tora,L. (2001) UV-damaged DNA-binding protein in the TFTC complex links DNA damage recognition to nucleosome acetylation. *EMBO. J.*, **20**, 3187–3196.
41. Martinez,E., Palhan,V.B., Tjernberg,A., Lymar,E.S., Gamper,A.M., Kundu,T.K., Chait,B.T. and Roeder,R.G. (2001) Human STAGA complex is a chromatin-acetylating transcription coactivator that interacts with pre-mRNA splicing and DNA damage-binding factors in vivo. *Mol. Cell Biol.*, **21**, 6782–6795.
42. Bai,R., Wan,R., Yan,C., Lei,J. and Shi,Y. (2018) Structures of the fully assembled Saccharomyces cerevisiae spliceosome before activation. *Science.*, **360**, 1423–1429.
43. Plaschka,C., Lin,P.C., Charenton,C. and Nagai,K. (2018) Prespliceosome structure provides insights into spliceosome assembly and regulation. *Nature.*, **559**, 419–422.
44. Stegeman,R., Spreacker,P.J., Swanson,S.K., Stephenson,R., Florens,L., Washburn,M.P. and Weake,V.M. (2016) The spliceosomal protein SF3B5 is a novel component of Drosophila SAGA that functions in gene expression independent of splicing. *J. Mol. Biol.*, **428**, 3632–3649.
45. Lesser,C.F. and Guthrie,C. (1993) Mutational analysis of pre-mRNA splicing in Saccharomyces cerevisiae using a sensitive new reporter gene, CUP1. *Genetics.*, **133**, 851–863.
46. Tang,Q., Rodriguez-Santiago,S., Wang,J., Pu,J., Yuste,A., Gupta,V., Moldon,A., Xu,Y.Z. and Query,C.C. (2016) SF3B1/Hsh155 HEAT motif mutations affect interaction with the spliceosomal ATPase Prp5, resulting in altered branch site selectivity in pre-mRNA splicing. *Genes. Dev.*, **30**, 2710–2723.
47. Shao,W., Kim,H.S., Cao,Y., Xu,Y.Z. and Query,C.C. (2012) A U1-U2 snRNP interaction network during intron definition. *Mol. Cell. Biol.*, **32**, 470–478.
48. Gornemann,J., Kotovic,K.M., Hujer,K. and Neugebauer,K.M. (2005) Cotranscriptional spliceosome assembly occurs in a stepwise fashion and requires the cap binding complex. *Mol. Cell*, **19**, 53–63.
49. Ewels,P.A., Peltzer,A., Fillinger,S., Patel,H., Alneberg,J., Wilm,A., Garcia,M.U., Di Tommaso,P. and Nahnsen,S. (2020) The nf-core framework for community-curated bioinformatics pipelines. *Nat. Biotechnol.*, **38**, 276–278.
50. Hvorecny,K.L. and Prelich,G. (2010) A systematic CEN library of the Saccharomyces cerevisiae genome. *Yeast.*, **27**, 861–865.
51. Eisenmann,D.M., Chapon,C., Roberts,S.M., Dollard,C. and Winston,F. (1994) The Saccharomyces cerevisiae SPT8 gene encodes a very acidic protein that is functionally related to SPT3 and TATA-binding protein. *Genetics*, **137**, 647–657.
52. Koutelou,E., Hirsch,C.L. and Dent,S.Y. (2010) Multiple faces of the SAGA complex. *Curr. Opin. Cell Biol.*, **22**, 374–382.
53. Exinger,F. and Lacroute,F. (1992) 6-Azauracil inhibition of GTP biosynthesis in Saccharomyces cerevisiae. *Curr. Genet.*, **22**, 9–11.
54. Dichtl,B., Blank,D., Ohnacker,M., Friedlein,A., Roeder,D., Langen,H. and Keller,W. (2002) A role for SSU72 in balancing RNA polymerase II transcription elongation and termination. *Mol. Cell*, **10**, 1139–1150.
55. Desmoucelles,C., Pinson,B., Saint-Marc,C. and Daignan-Fornier,B. (2002) Screening the yeast "disruptome" for mutants affecting resistance to the immunosuppressive drug, mycophenolic acid. *J. Biol. Chem.*, **277**, 27036–27044.
56. Samara,N.L. and Wolberger,C. (2011) A new chapter in the transcription SAGA. *Curr. Opin. Struct. Biol.*, **21**, 767–774.
57. Helmlinger,D. and Tora,L. (2017) Sharing the SAGA. *Trends Biochem. Sci.*, **42**, 850–861.
58. Zhou,K., Kuo,W.H., Fillingham,J. and Greenblatt,J.F. (2009) Control of transcriptional elongation and cotranscriptional histone modification by the yeast BUR kinase substrate Spt5. *Proc. Natl. Acad. Sci. U.S.A.*, **106**, 6956–6961.
59. Bian,C., Xu,C., Ruan,J., Lee,K.K., Burke,T.L., Tempel,W., Barsyte,D., Li,J., Wu,M., Zhou,B.O *et al.*2011) Sgf29 binds histone H3K4me2/3 and is required for SAGA complex recruitment and histone H3 acetylation. *EMBO. J.*, **30**, 2829–2842.
60. Belotserkovskaya,R., Sterner,D.E., Deng,M., Sayre,M.H., Lieberman,P.M. and Berger,S.L. (2000) Inhibition of TATA-binding protein function by SAGA subunits Spt3 and Spt8 at Gcn4-activated promoters. *Mol. Cell. Biol.*, **20**, 634–647.
61. Baptista,T., Grunberg,S., Minoungou,N., Koster,M.J.E., Timmers,H.T.M., Hahn,S., Devys,D. and Tora,L. (2017) SAGA Is a General Cofactor for RNA Polymerase II Transcription. *Mol. Cell.*, **68**, 130–143.
62. Talkish,J., Igel,H., Hunter,O., Horner,S.W., Jeffery,N.N., Leach,J.R., Jenkins,J.L., Kielkopf,C.L. and Ares,M. (2019) Cus2 enforces the first ATP-dependent step of splicing by binding to yeast SF3b1 through a UHM-ULM interaction. *RNA*, **25**, 1020–1037.
63. Perriman,R. and Ares,M. Jr. (2010) Invariant U2 snRNA nucleotides form a stem loop to recognize the intron early in splicing. *Mol. Cell.*, **38**, 416–427.
64. Rodgers,M.L., Tretbar,U.S., Dehaven,A., Alwan,A.A., Luo,G., Mast,H.M. and Hoskins,A.A. (2016) Conformational dynamics of stem II of the U2 snRNA. *RNA*, **22**, 225–236.
65. Zhang,Z.M., Yang,F., Zhang,J., Tang,Q., Li,J., Gu,J., Zhou,J. and Xu,Y.Z. (2013) Crystal Structure of Prp5p Reveals Interdomain Interactions that Impact Spliceosome Assembly. *Cell. Rep.*, **5**, 1269–1278.
66. Sermwittayawong,D. and Tan,S. (2006) SAGA binds TBP via its Spt8 subunit in competition with DNA: implications for TBP recruitment. *EMBO. J.*, **25**, 3791–3800.
67. Papai,G., Frechard,A., Kolesnikova,O., Crucifix,C., Schultz,P. and Ben-Shem,A. (2020) Structure of SAGA and mechanism of TBP deposition on gene promoters. *Nature*, **577**, 711–716.
68. Wang,H., Dienemann,C., Stutzer,A., Urlaub,H., Cheung,A.C.M. and Cramer,P. (2020) Structure of the transcription coactivator SAGA. *Nature*, **577**, 717–720.
69. Maudlin,I.E. and Beggs,J.D. (2019) Spt5 modulates co-transcriptional spliceosome assembly in Saccharomyces cerevisiae. *RNA*, **25**, 1298–1310.
70. Alexander,R.D., Innocente,S.A., Barrass,J.D. and Beggs,J.D. (2010) Splicing-dependent RNA polymerase pausing in yeast. *Mol. Cell*, **40**, 582–593.
71. Zhou,Q. and Sharp,P.A. (1996) Tat-SF1: cofactor for stimulation of transcriptional elongation by HIV-1 Tat. *Science*, **274**, 605–610.
72. Perriman,R. and Ares,M. Jr. (2000) ATP can be dispensable for prespliceosome formation in yeast. *Genes. Dev.*, **14**, 97–107.
73. Staley,J.P. and Guthrie,C. (1999) An RNA switch at the 5' splice site requires ATP and the DEAD box protein Prp28p. *Mol. Cell*, **3**, 55–64.
74. Murray,H.L. and Jarrell,K.A. (1999) Flipping the switch to an active spliceosome. *Cell*, **96**, 599–602.
75. Yang,F., Wang,X.Y., Zhang,Z.M., Pu,J., Fan,Y.J., Zhou,J., Query,C.C. and Xu,Y.Z. (2013) Splicing proofreading at 5' splice sites by ATPase Prp28p. *Nucleic Acids Res.*, **41**, 4660–4670.